Membrane protein thermodynamic stability may serve as the energy sink for sorting in the periplasm

C. Preston Moon, Nathan R. Zaccai, Patrick J. Fleming, Dennis Gessmann, and Karen G. Fleming[1]

T. C. Jenkins Department of Biophysics, The Johns Hopkins University, Baltimore, MD 21218

Edited* by Donald M. Engelman, Yale University, New Haven, CT, and approved January 24, 2013 (received for review July 20, 2012)

Thermodynamic stabilities are pivotal for understanding structure–function relationships of proteins, and yet such determinations are rare for membrane proteins. Moreover, the few measurements that are available have been conducted under very different experimental conditions, which compromises a straightforward extraction of physical principles underlying stability differences. Here, we have overcome this obstacle and provided structure–stability comparisons for multiple membrane proteins. This was enabled by measurements of the free energies of folding and the *m* values for the transmembrane proteins PhoP/PhoQ-activated gene product (PagP) and outer membrane protein W (OmpW) from *Escherichia coli*. Our data were collected in the same lipid bilayer and buffer system we previously used to determine those parameters for *E. coli* outer membrane phospholipase A (OmpLA). Biophysically, our results suggest that the stabilities of these proteins are strongly correlated to the water-to-bilayer transfer free energy of the lipid-facing residues in their transmembrane regions. We further discovered that the sensitivities of these membrane proteins to chemical denaturation, as judged by their *m* values, was consistent with that previously observed for water-soluble proteins having comparable differences in solvent exposure between their folded and unfolded states. From a biological perspective, our findings suggest that the folding free energies for these membrane proteins may be the thermodynamic sink that establishes an energy gradient across the periplasm, thus driving their sorting by chaperones to the outer membranes in living bacteria. Binding free energies of these outer membrane proteins with periplasmic chaperones support this energy sink hypothesis.

protein folding | protein sorting | protein stability

There has recently been a flood of new genetic and physiological revelations about biogenesis of microbial outer membranes in which a multiprotein complex built around the beta-barrel assembly machinery A (BamA) protein has been shown to be instrumental in integration of the nascent outer membrane β-barrel proteins (OMPs) into microbial outer membranes (1–3). This development promises to generate a much clearer picture of outer membrane biogenesis, which is critically important not only for our basic understanding of bacterial physiology but for many biological considerations, including bacterial pathogenesis, mammalian host tissue modification, and antibiotic resistance (4–6). Moreover, lessons about the maturation of bacterial OMPs are likely to be applicable to the outer membranes of mitochondria, which contain the sorting assembly machinery 50 kDa subunit (Sam50/Tob55), a BamA homolog (7, 8).

An intriguing question about microbial outer membrane biogenesis concerns the driving forces for sorting transmembrane β-barrels across the periplasm to the outer membranes. Because it is generally accepted that the periplasm lacks ATP or another obvious energy source (9), the energetics of OMP sorting are largely unknown except that the process is currently thought to be uncoupled from the proton motive gradient of the inner membrane. In the absence of an external energy source, an appealing hypothesis for driving this sorting is the existence of an energy sink located at the outer membrane. Because the folding of OMPs is the final step in their cellular biogenesis, one possibility is that their folding free energies serve as this thermodynamic sink. To more fully understand the energetic potentials available for β-barrel maturation in bacterial cell surfaces, we therefore sought to determine the thermodynamic stabilities of several outer membrane proteins. Since the thermodynamics of folding leads polypeptide chains to adopt a set of conformations that are at their equilibrium free energy minimum, a comparison of folding stabilities to the energetics of binding interactions that OMPs have with chaperones as they transit the periplasm to the outer membranes should reveal unique insights into the forces involved in the biogenesis of bacterial outer membranes (10–13).

Thermodynamic information describing the stabilities of OMPs is also a means to gain a more complete understanding of protein sequence–structure–function relationships because it enables a comparison of structural features and energetics of different protein sequences and folds. Because the energetics of a solvent are intimately linked to that of a protein folding within it, the most useful analysis would be formulated from membrane protein folding data collected in the same lipid bilayer environment. However, to date, the few stabilities available for membrane proteins have been measured under widely divergent lipid or micelle environments, complicating a straightforward extraction of general principles. Here, we address this problem by conducting thermodynamic measurements for a set of OMPs under identical buffer and lipid conditions.

Another key thermodynamic parameter extracted from protein folding studies is the equilibrium *m* value, defined as the sensitivity of the unfolding reaction to a particular denaturant. Even though this is an empirically observed constant, the *m* value has been shown to have physical meaning for water-soluble proteins and to correlate strongly with the difference in the extent of solvent (e.g., water) accessibility between the folded and unfolded conformations (14). For example, depressed *m* values can be used to infer that unfolded states have residual structure, that proteins are not fully unfolded, or that equilibrium folding data may be three-state even when it is apparently well described by two-state linear extrapolation equations. Although this type of information would be useful in the evaluation of membrane protein folding studies, no systematic analysis of membrane protein *m* values has yet been carried out to confirm whether the same correlation holds for them. In this study, we provide such data for a variety of OMPs from *E. coli*. We used these experimental results as a basis for comparison of stabilities and *m* values and to rationalize the biological implications stimulated by these data.

Author contributions: C.P.M., N.R.Z., P.J.F., and K.G.F. designed research; C.P.M., N.R.Z., P.J.F., and K.G.F. performed research; D.G. contributed new reagents/analytic tools; C.P.M., N.R.Z., P.J.F., and K.G.F. analyzed data; and C.P.M., N.R.Z., P.J.F., and K.G.F. wrote the paper.

The authors declare no conflict of interest.

*This Direct Submission article had a prearranged editor.

[1]To whom correspondence should be addressed. E-mail: karen.fleming@jhu.edu.

This article contains supporting information online at www.pnas.org/lookup/suppl/doi:10.1073/pnas.1212527110/-/DCSupplemental.

Results and Discussion

Our goals were to enable the extraction of information about sequence–structure–energy relationships for transmembrane proteins and to establish a reference point for energetic considerations of outer membrane biogenesis. To accomplish this, we chose to investigate the thermodynamic stabilities of a set of *E. coli* transmembrane proteins with known structures [outer membrane protein A (OmpA), OmpX, PhoP/PhoQ-activated gene product (PagP), OmpW, OmpT, and the long-chain fatty acid transport protein (FadL)]. These proteins all reside in the same biological membrane in vivo, and therefore any differences we observe in their folding behavior and/or conformational stabilities can be attributed to information contained within the polypeptide chain and not simply dismissed as arising from differences in their native lipid environments. In addition, we recently reported and have for comparison the thermodynamic stability of *E. coli* outer membrane phospholipase A (OmpLA) (15), which is found in the same biological membrane as the set above. Fig. S1 shows the known crystallographic structures of these seven OMPs aligned together in a schematic lipid bilayer revealing how these seven proteins range broadly in size with respect to both their apolar transmembrane domains and their polar water-exposed regions that extend outside of the bilayer.

Only OmpW and PagP Fold Reversibly: Other OMPs Show Hysteresis. Our ability to determine the folding free energy for OmpLA was only possible following an extensive, multivariable search for reversible, path-independent folding conditions (15, 16). To capitalize on this discovery, we sought to determine whether the particular condition we found for OmpLA would apply to other transmembrane proteins. All proteins in this set contain native tryptophan residues whose fluorescence emission we used to monitor their conformational equilibria. In screening, we monitored the wavelength of maximum emission, λ_{max}, because it is technically easier to collect. Although λ_{max} is not linearly related to population, it is still the case that unfolding and refolding curves must overlay for equilibrium constraints to be satisfied. Fig. S2 shows these data where it can be observed that only OmpW and PagP display path-independent unfolding and refolding curves that exactly overlay upon each other: all other proteins display hysteresis under these conditions. The presence of a hysteresis loop indicates that one or both processes face an insurmountable activation barrier to equilibrium within the 36-h time period of the experiment. Unfortunately, it is not possible from these data to know whether either the folding or the unfolding or both transitions impose this activation barrier to equilibrium.

Notably, hysteresis is not a flaw of our experimental setup but has been previously been reported for OmpA, PagP, and OmpLA under different conditions (16–19). We collected light scattering signals during our fluorescence experiments to confirm that aggregation was not a causal factor (Fig. S3). In a further attempt to find a structural parameter that could explain this hysteresis, we quantified the extent of hysteresis by taking the difference between the areas under the curves, and we compared it to a number of geometric and physical parameters: the change in accessible surface area (ΔASA) upon folding, the ratio of water exposed mass to lipid-buried mass, or the calculated charge (Fig. S4). No correlations were found.

Like OmpLA, the Stabilities of OmpW and PagP Are Quite Large. We next collected fluorescence intensity data at 330 nm for OmpW and PagP because this observable is linearly proportional to population, and such data can be fitted using the linear extrapolation model to obtain an estimate for the folding free energy in the absence of denaturant. Shown in Fig. 1 and Fig. S5, the data for both proteins are well described by a two-state folding equation from which we obtained best-fit values of 18.3 (±0.5) and 24.4 (±0.4) kcal·mol^{-1} for the free energies of unfolding in the absence of denaturant and 4.5 (±0.1) and 5.4 (±0.1) kcal·mol^{-1}·M^{-1} guanidine hydrochloride (GdnHCl) for the *m* values for OmpW and PagP, respectively.

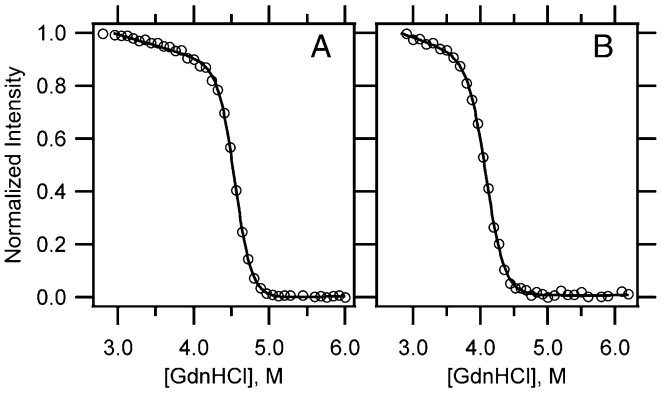

Fig. 1. The reversible transitions of PagP and OmpW are two-state when titrated with guanidine HCl. Data points represent measurements of tryptophan fluorescence emission intensity at 330 nm, normalized such that the emission intensity from folded protein at the lowest guanidine HCl concentration is 1 and the emission intensity from unfolded protein is 0. The excitation wavelength was 295 nm. The solid lines represent fits of the data to a two-state linear extrapolation model. (*A*) Example titration data for PagP. (*B*) Example titration data for OmpW.

This is the first measurement of the OmpW stability, but we can compare our PagP stability with that previously reported by Huysmans et al. (19) Even though the bilayer environment is the same [1,2-dilauroyl-*sn*-glycero-3-phosphocholine (DLPC) large unilamellar vesicles (LUVs)], our measure of the PagP conformational stability is ∼10 kcal·mol^{-1} more favorable than previously reported. Nevertheless, we think the two results are not incompatible, and we largely attribute the discrepancies in these values to differences in the denaturant used and its subsequent impact on the denatured state ensemble. Huysmans et al. used urea as the denaturant, whereas we used GdnHCl, which is known to be twofold to threefold stronger in denaturing soluble proteins (20). In addition, urea is thought to allow some structure in the denatured state ensemble that is increased in soluble proteins having greater numbers of nonpolar residues (21). This can mean that the denatured state ensemble conformation is not fully unfolded. In accordance with this idea, Huysmans et al. found the denatured state ensemble of PagP to be partitioned onto the surface of their lipid bilayers (19), and the free energy change they report thus corresponds to a bilayer surface-to-inserted transition. This is quite different from our denaturation studies in which we observe the denatured state ensemble of PagP to be free in solution, i.e., not bound to the membrane surface. In accordance with the distinctions in the unfolded states, we obtain a value of −10.74 kcal·mol^{-1} when we use the Wimley–White interfacial scale to predict the partitioning free energy of the PagP sequence from water to the surface of a phosphatidylcholine bilayer. This number completely accounts for and can explain the PagP stability differences observed between our group and Huysmans et al.

Free Energy of Folding May Be an Energy Sink for Sorting in the Periplasm. Like OmpLA, whose unfolding free energy change was found to be 32.5 kcal·mol^{-1}, the thermodynamic stabilities of OmpW and PagP are quite high compared with soluble proteins of similar molecular weight. Because evolutionary pressures optimize proteins for function, these robust values raise interesting biological questions about what functional role(s) may be linked to these folding free energies. We propose that one biological rationale for such high thermodynamic stabilities is that the OMP free energy of folding serves as the energy sink for the cellular

sorting process that sends transmembrane β-barrel proteins to bacterial outer membranes. Unlike the cytoplasm where the energy of ATP is available for ensuring efficient protein folding, no obvious external energy source is present in the periplasm for this process, which, moreover, is currently thought to be uncoupled from the chemical potential of the inner membrane. The robust folding free energies for OMPs represent a deep energy well that could facilitate an efficient free energy gradient of sequential molecular association events that starts with an OMP's interactions with chaperones upon emergence of the nascent chain from the translocon.

For this process to be ultimately driven by the OMP folding free energy, it must be the case that all previous interactions of unfolded OMPs be less energetically favorable so that the energy flow will be "downhill" as nascent OMP chains proceed to the outer membrane and assume their native conformations. Fig. 2 shows a schematic that summarizes the known binding interactions of a nascent OMP polypeptide chain after it enters the periplasm through the translocon. Genetic experiments indicate that the periplasmic chaperones seventeen kilodalton protein (Skp) and survival protein A (SurA) both play roles in the biological maturation of OMPs (11, 22–24). Consistent with a thermodynamic driving force for periplasmic sorting, Fig. 3 shows that binding of the Skp trimer (Skp_T) to unfolded OmpLA, PagP, or OmpW ranges from −10.8 to −11.8 kcal·mol^{-1}, which is far less favorable than the thermodynamic stabilities of these folded proteins in membranes. The Skp or SurA binding data to several other unfolded OMPs (uOMPs) determined previously by two independent groups indicate that the energetics of chaperone/uOMP interactions are similar (10, 13). It is currently unknown whether Skp and SurA show client specificity, but they must be somewhat functionally redundant because the phenotypes for single deletions are relatively mild, whereas the Δ*skp*/Δ*surA* phenotype is synthetic lethal (23–25). uOMPs can also interact with periplasmic serine endoprotease DegP (DegP) (13). Formation of this complex is slightly more stable than the interactions uOMPs have with Skp or SurA; however, binding of uOmpC to DegP has been shown to be 1,000 times slower, giving Skp and SurA a kinetic advantage in their binding (13). uOMPs are also known to self-associate to form very large complexes in vitro (26). The free energy of this interaction has been estimated as −9.1 kcal·mol^{-1} for unfolded OmpA (27). Although each of these reactions represents a significant use of cellular free energy in the periplasm, the OMP folding free energies are still much more favorable than any of these known uOMP/chaperone interactions. This energy difference ensures OMP transit across the periplasm and incorporation into outer membranes in the absence of an external energy source.

A second biological implication arising from the OMP thermodynamic stabilities relates to the cellular lifetimes of outer transmembrane β-barrels. The robust stabilities of OMPs allow one to predict that—once folded—their unfolded conformations

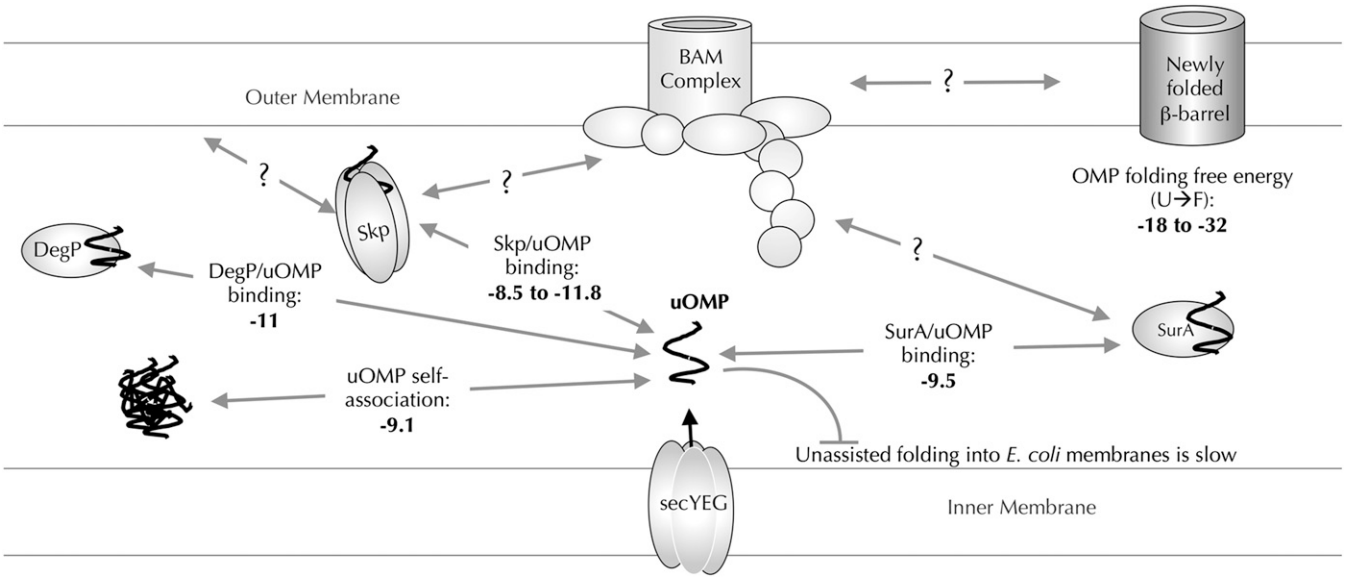

Fig. 2. Schematic of known thermodynamic parameters for periplasmic folding of outer membrane proteins. All numbers in this schematic are binding free energies measured in vitro reported in kilocalories per mole. Nascent OMPs, shown as a bold squiggle line, enter the periplasm in unfolded conformations. Upon emerging from the translocon, they are thought to enter the folding pathway by interacting with Skp or SurA with binding free energies in the range −8.5 to −11.8 kcal·mol^{-1} (1, 10). Deletion of either *skp* or *surA* results in reduced levels of mature OMPs in outer membranes, and this is attributed to OMP interactions with DegP (13). Although DegP binds uOMPs with a more favorable free energy (13) (as indicated), its interaction with uOMPs is ∼1,000-fold slower than those of Skp or SurA (13). uOMP self-association is another binding reaction with approximately the same free energy of formation as uOMP/chaperone interactions; for OmpA, this has been shown to be −9.1 kcal·mol^{-1} measured under conditions similar to those reported for the uOMP/chaperone interactions (27). The rate of uOMP self-association is not currently known, but we anticipate it to be slower than the rate of uOMP binding to Skp or SurA based on the observation that Skp can prevent the aggregation of unfolded OMPs (12). Similarly, the in vitro folding of OMPs significantly slows as the bilayer thickness approaches that of biological membranes (33), and folding occurs with low efficiency using membranes derived from *E. coli* (33), thus suggesting that *E. coli* membranes present a kinetic barrier to folding as a negative selection against incorporation into bacterial inner membranes. A key unknown in this scheme is the interaction energy with the outer membrane beta-barrel assembly machinery (BAM complex) that is known to be important for efficient OMP folding in cells and whose components are essential in *E. coli* (38, 39). SurA is thought to participate in BAM-assisted folding of uOMPs (40), but the energy of this interaction is unknown as indicated by the question mark. Additionally, the biological fate of a uOMP/Skp complex is not well understood. In vitro, OMPs can refold starting from a uOMP/Skp complex (41), but it is not clear whether this happens in vivo or whether uOmp/Skp also has interactions with the BAM complex. Importantly, all known interactions have binding free energies that are significantly less favorable than the free energies of OMP folding. The uOmpA self-association free energy was calculated from the linear extrapolation of the midpoint concentration of the monomer-nMer reaction measured as a function of total urea concentration [figure 5*C* in Danoff and Fleming (27); slope = 9.2E-6; intercept = 1.8E-7]. The value of −9.1 corresponds to the condition of buffer containing 80 mM urea to be equivalent to that used in the chaperone binding measurements in this study and that of Wu et al. (13).

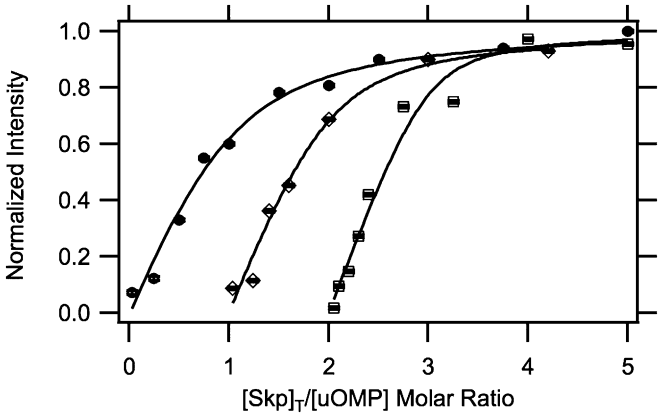

Fig. 3. The Skp_T binding to uOmpLA, uOmpW, or uPagP is less energetically favorable than the folding free energies of these proteins. Typical binding isotherms describing the binding of uOmpLA (circles), uOmpW (diamonds), or uPagP (squares) determined using the uOMP intrinsic fluorescence intensity at 341 nm. The [uOMP] was held constant for each titration and equaled 40, 25, and 20 nM for OmpLA, OmpW, and PagP, respectively, while titrating in various molar ratios of Skp_T. The error bars represent the error of the signal and are smaller than the symbol size. Each isotherm was measured a minimum of three times, and the average dissociation constants were found to be 10.8 ± 0.2 nM (Skp_T/uOmpLA); 11.3 ± 0.2 nM (Skp_T/uOmpW); and 11.8 ± 0.3 nM (Skp_T/uPagP). For clarity, the uOmpW and uPagP data are offset by 1 and 2 molar ratio units on the abscissa, respectively.

will be unpopulated under cellular conditions because the unfolding rates for these membrane proteins will be quite slow. Even without knowing the full height of the activation free energy barrier to unfolding, we know from the thermodynamic stabilities of OMPs that it must at least be equal to the equilibrium values, e.g., 18–32 kcal·mol^{-1}. This finding is consistent with kinetic studies on bacteriorhodopsin in which the extrapolated unfolding rate from micelles in the absence of denaturant was found to equal ~10^{-15} s^{-1}—more than a million years (28)! Thus, in addition to robust thermodynamic stability, which serves as the energy sink for periplasmic sorting, membrane proteins display significant kinetic stability. Although such slow unfolding would normally imply the existence in the cell of an active mechanism for degradation of membrane proteins, the problem of accumulating aged outer membrane proteins may be solved in Gram-negative bacteria by dilution due to bacterial division and/or by the blebbing off of outer membrane minivesicles (29–31). Moreover, a biological explanation for evolutionary optimization of such high kinetic stability may be to allow OMPs to withstand the harsh extracellular environment of the outer membrane.

Membrane Protein Stability Is Correlated to the Water-to-Bilayer Transfer Free Energy of Acyl-Contact Residues. From a biophysical perspective, it is worth considering how OMPs may achieve such high thermodynamic stabilities, and the availability of these three stability measurements under identical lipid and buffer conditions offers opportunities for sequence–structure–energy correlations. We therefore examined a number of structural parameters for correlation with total thermodynamic stability, including molecular weight, number of β strands, number of residues buried in the bilayer (which should correlate with the number of lipid-buried peptide bonds), total ΔASA upon folding, and fraction of total ASA buried in the lipid bilayer. None of these showed strong trends that could be discerned with the current dataset. In particular, PagP has a lower molecular weight than OmpW but is significantly more stable, an unexpected finding if size was a sole determinant of stability.

The only relationship we observed was a linear correlation between overall stability and the water-to-bilayer transfer free energy of acyl-contacting side chains. Shown in Fig. S6, we observed a remarkable Pearson coefficient for this linear regression ($R = 0.9999$). Of course, we recognize that this finding should be received with some skepticism because the number of data points is limiting and the significance remains to be tested; even so, this result does proffer a rational strategy to tune the total membrane protein stability by alteration of the side chains on its lipid-facing surface. More fundamentally, this initial correlation, if it bears the test of time, suggests that large and opposing energetic terms combine to define a membrane protein's thermodynamic stability: Approximately 5 kcal·mol^{-1} of acyl-contact side-chain insertion energy corresponds to each kilocalorie per mole of total stability, which means that 4 kcal·mol^{-1} per acyl-contact residue must oppose the folded conformation in membranes. Notably, we speculate that this energy term must involve more than the penalty of partitioning the hydrogen bonded peptide bond into the bilayer, as this energy should scale with the number of those groups buried, and it cannot account for the opposing energy values in these three proteins. To examine the acyl-contacting side chains in greater detail, we plotted their frequencies in Fig. S7. This shows that OmpLA buries about double the number of Leu side chains compared with either OmpW or PagP (20 versus 5 and 8, respectively). From this, one might expect that hydrophobicity should explain the correlation in Fig. S6, but this does not appear to be the case because regressing the nonpolar surface area of these acyl-contacting residues against the total stability does not recapitulate the linear relationship with the same Pearson coefficient ($R = 0.70$).

***m* Values of These Transmembrane Proteins Follow the *m* Value Dependence on ΔASA_{Fold} Previously Observed for Soluble Proteins.** In addition to the thermodynamic stability, chemical denaturation experiments provide estimates of the denaturant *m* value, defined as the dependence of the change in free energy of unfolding on denaturant concentration. Although *m* is an empirically observed parameter obtained from the linear extrapolation fitting procedure, Myers et al. (14) discovered a physical meaning for its magnitude. By analyzing the folding data for 45 soluble proteins, they demonstrated that *m* values followed a linear relationship with the predicted change in solvent accessible surface area upon unfolding, ΔASA. At first glance the *m* values for OmpLA, OmpW, and PagP are high compared with soluble proteins of similar molecular weights, but this can be explained by the fact that OMP folded

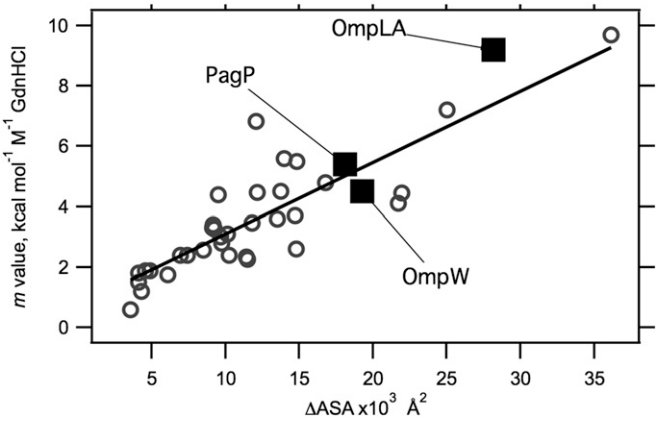

Fig. 4. *m* values for transmembrane proteins follow the same dependence on ΔASA as soluble proteins. Shown in open circles are the GdnHCl data from table 1 of Myers et al. (14). The values for PagP, OmpW, and OmpLA are overlaid upon the data of Myers et al. and are not included in the linear correlation.

conformations bury a significant fraction of their surface residues in the hydrophobic regions of bilayers and thus exclude more surface area from water upon folding than do soluble proteins of comparable molecular weights. When this excess buried ΔASA is taken into account, we find that the *m* values for these three OMPs are well within the distribution previously observed (Fig. 4). We speculate that this result means that the mechanism by which GdnHCl unfolds proteins is conserved between membrane and soluble proteins to the extent that their denatured state ensembles may share denaturant induced conformational features. As with soluble proteins, this *m* value correlation should be useful in evaluating chemical denaturation experiments to evaluate whether membrane proteins are fully unfolded or whether folding/unfolding titration data might really be three-state even when it is apparently well described by two-state linear extrapolation equations, because both of these situations will lead to *m* values lower than expected.

Moreover, the observation that the *m* values in this study are well explained by the Myers et al. correlation is consistent with a previous proposal by Hong and Tamm (32) regarding *m* values for OmpA observed as a function of bilayer thickness. They proposed that the *m* value reflected the bilayer lateral pressure when the bilayer thickness was mismatched to that of OmpA. Since the hydrophobic thickness of the bilayer in the current study is well matched to that of the transmembrane regions of the OMPs we investigated (37), the excess lateral pressure due to hydrophobic mismatch is not an important parameter here. In addition, our thermodynamic measurements were carried out using large unilamellar vesicles. These lack the additional curvature strain arising from the small unilamellar vesicles used by Hong and Tamm, which the authors stated might be another contributing factor in those studies.

In summary, our measurements for membrane protein stabilities stimulate many biophysical questions about the physical basis for protein folding. Our preliminary structure–energy correlation indicates that, like soluble proteins, large and opposing forces are involved in stabilizing membrane proteins. If this correlation is supported by future experimental results, it should find practical utility in the design of membrane proteins with altered stabilities because these can be constructed by taking the transfer free energies of lipid-facing residues into account. Biologically, our results provide evidence that membrane protein thermodynamic stability may be an important energy source in the maturation of bacterial cell envelopes. At the same time, the kinetic stabilities of OMPs ensure that the transmembrane proteins in bacterial cell surfaces can withstand the harsh environments of extracellular milieu.

Materials and Methods

Protein Folding and Unfolding Denaturant Titrations. All proteins were cloned and expressed to inclusion bodies as previously described (33). For folding and unfolding titrations, we followed the protocol we previously used to measure the thermodynamics of OmpLA (15, 16). This is described in greater detail in *SI Text*.

Measurement of Folding Free Energies and *m* Values. We fit the titration data for PagP and OmpW in Fig. 1 with the standard two-state linear extrapolation model (20) using Igor Pro, version 6.12 (WaveMetrics), and allowing all parameters of the fit to vary. For each protein, we fit four independent titrations made from independent protein, lipid, and buffer preparations, and we averaged the results to arrive at the parameters shown in Table S1.

Measurement of Skp_T Binding to uOMPs. The change in uOMP intrinsic tryptophan fluorescence intensity was used to measure the binding of each uOMP to Skp_T. The background fluorescence of Skp_T was measured at each concentration followed by the addition of uOMP from an 8 M solution to achieve a final buffer condition of 20 mM Tris, pH 8.0, 80 mM urea. The experimental data were fitted using a single site, tight binding equation in which one Skp_T binds per uOMP. This is described in greater detail in *SI Text*.

PagP Bilayer Surface Partitioning. We used the Wimley–White whole-residue interfacial scale (34, 35) and the amino acid composition of PagP to calculate the predicted partitioning free energy from water to the bilayer surface. Because our experimental pH is 3.8, we used the protonated whole-residue values for Asp, Glu, and His.

Calculation of ΔASA Values. We used the program calc-surf with a default probe size of 1.4 Å for all ASA calculations (36). The change in total ASA upon unfolding was calculated by taking the difference in water ASA between unfolded (Coord #01) and folded conformations embedded in only the acyl chains of a DLPC bilayer (Coord #02). For the unfolded models, we used Pymol to build extended structures ($\phi = -78°$; $\psi = 149°$) of the corresponding sequences, termed Coord #01. We used this model for direct comparison with the data of Myers et al. (14), who modeled unfolded states as extended. However, we recognize that this is probably not a fully realistic representation of the unfolded conformation as indicated by our hydrodynamic measurements of the unfolded conformation of OmpA (27). To calculate water ASA for the folded conformation, we used five uncorrelated snapshots from the trajectories of the membrane-embedded, equilibrated folded state in DLPC bilayers as a starting point. Because interfacial and headgroup regions of bilayers are hydrated, we used scripts to remove the DLPC head group atoms and used the resultant coordinates of the acyl-embedded protein and acyl chain system (Coord #02) as input into calc-surf.

Determination of Acyl Contact Residues. We used ASA calculations to enumerate those residues in contact with the lipid acyl chains and not accessible to water. We used five snapshots of the trajectories of membrane embedded, equilibrated folded states in DLPC bilayers as a starting point for these calculations. We first generated a coordinate file for a virtual folded protein in water by removing all nonprotein atoms (Coord #3) and calculated the water ASA for this virtual protein. We subtracted each atom's ASA of Coord #2 from Coord #3 to obtain a list of those atoms that become shielded from water upon insertion into the bilayer. We summed this ASA difference for each residue and counted the residue as a "lipid exposed" if its sum was >10 $Å^2$. These are the residue frequencies shown in Fig. S7. We used the Moon–Fleming hydrophobicity scale (15) to calculate the total free energy of transfer for this list of side chains for each protein and report the average value of the calculations for the five trajectory snapshots.

Molecular Dynamics Simulations for PagP and OmpW. The molecular dynamics calculations of OmpLA have been previously published (37). A similar protocol was used for PagP and OmpW in DLPC bilayers and is described in detail in *SI Text*.

ACKNOWLEDGMENTS. This work was supported by National Science Foundation Grants MCB0423807 and MCB0919868, and National Institutes of Health Grants R01 GM079440 and T32 GM008403.

1. Wu T, et al. (2005) Identification of a multicomponent complex required for outer membrane biogenesis in *Escherichia coli*. *Cell* 121(2):235–245.
2. Sklar JG, et al. (2007) Lipoprotein SmpA is a component of the YaeT complex that assembles outer membrane proteins in *Escherichia coli*. *Proc Natl Acad Sci USA* 104(15):6400–6405.
3. Kim S, et al. (2007) Structure and function of an essential component of the outer membrane protein assembly machine. *Science* 317(5840):961–964.
4. Meyer AL (2005) Prospects and challenges of developing new agents for tough Gram-negatives. *Curr Opin Pharmacol* 5(5):490–494.
5. Wilson M (2004) *Microbial Inhabitants of Humans* (Cambridge Univ Press, Cambridge, UK), p 476.
6. Otto K, Hermansson M (2004) Inactivation of ompX causes increased interactions of type 1 fimbriated *Escherichia coli* with abiotic surfaces. *J Bacteriol* 186(1):226–234.
7. Kozjak V, et al. (2003) An essential role of Sam50 in the protein sorting and assembly machinery of the mitochondrial outer membrane. *J Biol Chem* 278(49):48520–48523.
8. Kutik S, et al. (2008) Dissecting membrane insertion of mitochondrial beta-barrel proteins. *Cell* 132(6):1011–1024.
9. Wülfing C, Plückthun A (1994) Protein folding in the periplasm of *Escherichia coli*. *Mol Microbiol* 12(5):685–692.
10. Qu J, Mayer C, Behrens S, Holst O, Kleinschmidt JH (2007) The trimeric periplasmic chaperone Skp of *Escherichia coli* forms 1:1 complexes with outer membrane proteins via hydrophobic and electrostatic interactions. *J Mol Biol* 374(1):91–105.
11. Schäfer U, Beck K, Müller M (1999) Skp, a molecular chaperone of Gram-negative bacteria, is required for the formation of soluble periplasmic intermediates of outer membrane proteins. *J Biol Chem* 274(35):24567–24574.

12. Walton TA, Sandoval CM, Fowler CA, Pardi A, Sousa MC (2009) The cavity-chaperone Skp protects its substrate from aggregation but allows independent folding of substrate domains. *Proc Natl Acad Sci USA* 106(6):1772–1777.
13. Wu S, et al. (2011) Interaction between bacterial outer membrane proteins and periplasmic quality control factors: A kinetic partitioning mechanism. *Biochem J* 438(3): 505–511.
14. Myers JK, Pace CN, Scholtz JM (1995) Denaturant m values and heat capacity changes: Relation to changes in accessible surface areas of protein unfolding. *Protein Sci* 4(10): 2138–2148.
15. Moon CP, Fleming KG (2011) Side-chain hydrophobicity scale derived from transmembrane protein folding into lipid bilayers. *Proc Natl Acad Sci USA* 108(25): 10174–10177.
16. Moon CP, Kwon S, Fleming KG (2011) Overcoming hysteresis to attain reversible equilibrium folding for outer membrane phospholipase A in phospholipid bilayers. *J Mol Biol* 413(2):484–494.
17. Pocanschi CL, Patel GJ, Marsh D, Kleinschmidt JH (2006) Curvature elasticity and refolding of OmpA in large unilamellar vesicles. *Biophys J* 91(8):L75–L77.
18. Sanchez KM, Gable JE, Schlamadinger DE, Kim JE (2008) Effects of tryptophan microenvironment, soluble domain, and vesicle size on the thermodynamics of membrane protein folding: Lessons from the transmembrane protein OmpA. *Biochemistry* 47(48):12844–12852.
19. Huysmans GH, Baldwin SA, Brockwell DJ, Radford SE (2010) The transition state for folding of an outer membrane protein. *Proc Natl Acad Sci USA* 107(9):4099–4104.
20. Santoro MM, Bolen DW (1988) Unfolding free energy changes determined by the linear extrapolation method. 1. Unfolding of phenylmethanesulfonyl alpha-chymotrypsin using different denaturants. *Biochemistry* 27(21):8063–8068.
21. Nick Pace C, et al. (2010) Urea denatured state ensembles contain extensive secondary structure that is increased in hydrophobic proteins. *Protein Sci* 19(5):929–943.
22. Behrens S, Maier R, de Cock H, Schmid FX, Gross CA (2001) The SurA periplasmic PPIase lacking its parvulin domains functions in vivo and has chaperone activity. *EMBO J* 20(1-2):285–294.
23. Lazar SW, Kolter R (1996) SurA assists the folding of *Escherichia coli* outer membrane proteins. *J Bacteriol* 178(6):1770–1773.
24. Missiakas D, Betton JM, Raina S (1996) New components of protein folding in extracytoplasmic compartments of *Escherichia coli* SurA, FkpA and Skp/OmpH. *Mol Microbiol* 21(4):871–884.
25. Rizzitello AE, Harper JR, Silhavy TJ (2001) Genetic evidence for parallel pathways of chaperone activity in the periplasm of *Escherichia coli*. *J Bacteriol* 183(23):6794–6800.
26. Ebie Tan A, Burgess NK, DeAndrade DS, Marold JD, Fleming KG (2010) Self-association of unfolded outer membrane proteins. *Macromol Biosci* 10(7):763–767.
27. Danoff EJ, Fleming KG (2011) The soluble, periplasmic domain of OmpA folds as an independent unit and displays chaperone activity by reducing the self-association propensity of the unfolded OmpA transmembrane β-barrel. *Biophys Chem* 159(1): 194–204.
28. Curnow P, Booth PJ (2007) Combined kinetic and thermodynamic analysis of alpha-helical membrane protein unfolding. *Proc Natl Acad Sci USA* 104(48):18970–18975.
29. Beveridge TJ (1999) Structures of Gram-negative cell walls and their derived membrane vesicles. *J Bacteriol* 181(16):4725–4733.
30. Henry T, et al. (2004) Improved methods for producing outer membrane vesicles in Gram-negative bacteria. *Res Microbiol* 155(6):437–446.
31. Kadurugamuwa JL, Beveridge TJ (1995) Virulence factors are released from *Pseudomonas aeruginosa* in association with membrane vesicles during normal growth and exposure to gentamicin: A novel mechanism of enzyme secretion. *J Bacteriol* 177(14): 3998–4008.
32. Hong H, Tamm LK (2004) Elastic coupling of integral membrane protein stability to lipid bilayer forces. *Proc Natl Acad Sci USA* 101(12):4065–4070.
33. Burgess NK, Dao TP, Stanley AM, Fleming KG (2008) Beta-barrel proteins that reside in the *Escherichia coli* outer membrane *in vivo* demonstrate varied folding behavior *in vitro*. *J Biol Chem* 283(39):26748–26758.
34. White SH, Wimley WC (1999) Membrane protein folding and stability: Physical principles. *Annu Rev Biophys Biomol Struct* 28:319–365.
35. Wimley WC, White SH (1996) Experimentally determined hydrophobicity scale for proteins at membrane interfaces. *Nat Struct Biol* 3(10):842–848.
36. Gerstein M, Chothia C (1996) Packing at the protein-water interface. *Proc Natl Acad Sci USA* 93(19):10167–10172.
37. Fleming PJ, Freites JA, Moon CP, Tobias DJ, Fleming KG (2012) Outer membrane phospholipase A in phospholipid bilayers: A model system for concerted computational and experimental investigations of amino acid side chain partitioning into lipid bilayers. *Biochim Biophys Acta* 1818(2):126–134.
38. Ricci DP, Silhavy TJ (2012) The Bam machine: A molecular cooper. *Biochim Biophys Acta* 1818(4):1067–1084.
39. Ricci DP, Hagan CL, Kahne D, Silhavy TJ (2012) Activation of the *Escherichia coli* β-barrel assembly machine (Bam) is required for essential components to interact properly with substrate. *Proc Natl Acad Sci USA* 109(9):3487–3491.
40. Hagan CL, Kim S, Kahne D (2010) Reconstitution of outer membrane protein assembly from purified components. *Science* 328(5980):890–892.
41. Bulieris PV, Behrens S, Holst O, Kleinschmidt JH (2003) Folding and insertion of the outer membrane protein OmpA is assisted by the chaperone Skp and by lipopolysaccharide. *J Biol Chem* 278(11):9092–9099.